JOURNAL OF GEOPHYSICAL RESEARCH, VOL. 106, NO. D24, PAGES 33,773–33,780, DECEMBER 27, 2001

A new ice thickness and bed data set for the Greenland ice sheet
1. Measurement, data reduction, and errors

J. L. Bamber and R. L. Layberry

Bristol Glaciology Centre, School of Geographical Sciences, University of Bristol, England, United Kingdom

S.P. Gogineni

Radar Systems and Remote Sensing Laboratory, University of Kansas, Lawrence, Kansas

Abstract. Ice thickness data collected between 1993 and 1999 using a coherent ice-penetrating radar system developed at the University of Kansas have been combined with data collected by the Technical University of Denmark in the 1970s to produce a new ice thickness grid for Greenland. Crossover analysis was used to assess the relative accuracy of the two data sets and they were weighted accordingly and interpolated onto a regular 5-km spacing grid using a kriging interpolation procedure. A high-resolution land-ice mask was used to help constrain the interpolation of the ice thickness data near the ice sheet margins where, in the past, the relative errors have been largest. The ice thickness grid was combined with a new digital elevation model of the ice sheet and surrounding rock outcrops to produce a new bed elevation data set for the whole of Greenland. The ice thickness grid was compared with the currently available data set. Differences in the center of the ice sheet, where the ice is thickest, were of the order of a few percent. Near the margins, however, large differences, of as much as a factor of 10, were found. The total volume of ice contained in the ice sheet was reestimated and found to have a value of 2.93×10^6 km^3. The ice thickness grid was used to calculate the spatial pattern of gravitational driving stress over the ice sheet. Anomalous patterns of stress were found in areas that appeared to be associated with areas of rapid flow.

1. Introduction

Ice thickness and bedrock topography are essential boundary conditions for numerical modeling studies of the Greenland ice sheet. The existing ice thickness data set available for such applications was generated about a decade ago from data collected during the 1970s [*Letreguilly et al.*, 1991], henceforward called the Letreguilly grid. With recent improvements in the quality of other boundary conditions (such as ice surface elevation and accumulation) the accuracy of this data set now poses a serious limitation to reliable simulations of the ice sheet's dynamics and future behavior. In this paper, we present a new ice thickness and bed elevation data set that addresses this limitation.

In 1991 a research effort to measure the surface elevation of Greenland using laser altimeter data began as part of a wider effort to determine the mass balance of the ice sheet. In 1993 a 150-MHz ice-penetrating radar (IPR), developed and operated by the Remote Sensing Laboratory at the University of Kansas, was included on the airborne survey, and since 1993 and up to and including 1999, yearly surveys have yielded a wealth of ice thickness data which have been disseminated for general use [*Gogineni et al.*, this issue].

Paper number 2001JD900054.
0148-0227/01/2001JD900054$09.00

Here we report on the use of these thickness data, in conjunction with a data set collected during the 1970s and the latest surface digital elevation model (DEM), to interpolate a new ice thickness and bedrock grid for the ice sheet. The data from the 1970s is of markedly lower quality but is, nonetheless, useful in filling in gaps in coverage in the 1990s data, and its lower accuracy is accounted for in this study.

2. Data Analysis

The primary data set used in this study is the IPR data collected by the University of Kansas. Here we describe the key attributes of the radar system (discussed in greater detail in *Gogineni et al.*, this issue) and the methodology adopted for processing these data.

2.1. Kansas Radar System

The coherent IPR system transmitted a 150-MHz chirped, 1.6-μs pulse with a peak power of 200 W. The equipment and various improvements to it are described in detail by *Gogineni et al.* [1998, *this issue*]. Aircraft navigation employed kinematic GPS and a precision laser altimeter system. The separate transmit and receive antenna consisted of a four-element, half-wavelength dipole array. The returned signal was amplified with an end-to-end gain of 95 dB and had a resolution in ice of 5 m. The signal was detected coherently, providing in-phase and quadrature components which were digitized at a sample rate of 18.75×10^6 samples per second.

Integration was performed over 256 consecutive pulses, and the power in each record was computed before being further integrated over four data records.

The depth of the bedrock was computed by the number of pixels between the top and the bedrock return, with each pixel representing 4.494 m of travel though the ice. The higher radio wave velocity through the upper firn layer compared with solid ice was compensated for by adding 10 m to the estimated ice thickness, as is common practice for ice sheets with a relatively deep firn layer [*Bogorodskiy and Bentley*, 1985]. The returns were picked manually, providing an initial quality control. This was performed at the University of Kansas, and it was in this form that the results were made available.

The data from the 1970s were collected by the Technical University of Denmark using a 60-MHz echo sounder, analogue recording technology, and an inertial navigation system [*Bogorodskiy and Bentley*, 1985]. These data were provided already fully processed and edited as latitude (y), longitude (x) and thickness (z).

2.2 Data Extent, Quality, and Filtering

The 1970s and 1990s flight lines are shown in Figure 1. Both data sets are extensive, though the along-track sampling from the 1970s was significantly coarser (average spacing 1 km) compared with 1990s data (average spacing 150 m). In all, the 1970s data contained ~ 30,000 thickness data points, and the 1990s data contained almost 700,000 data points.

The across-track spacing is highly variable but is typically of the order of 20 km. In the vicinity of the airfields that were used for the field surveys (Thule and Søndre Strømfjord), the tracks are relatively dense, while parts of the southern tip of the ice sheet have gaps of as much as 120 km between tracks.

Crossover analysis was used to assess the accuracy of the data sets, both for internal consistency and for consistency between data sets. The 1970s data had an average crossover difference of 130 m, due primarily to errors in the navigation data. The 1990s data had an average crossover anomaly of 15 m. There were, however, some 1990s tracks which were removed, as there were some problems with matching the radar data to the navigation data. These manifested themselves, for example, as different thicknesses with identical positions.

The data were averaged locally in a polar stereographic coordinate system using a linear distance weighting method, resulting in a quasi-regular, 301 by 561 array of mean x, y and z with roughly 5-km spacing. The thickness, z, at each grid point was given by the weighted average of the data within the search radius of the cell center and the mean x and y values were given by the similarly weighted averages of the positions of each radar data point. The 1990s data were given a factor of 10 higher weighting relative to the 1970s data, on the basis of the crossover analysis. This initial averaging of the data reduced the number of points used in the final interpolation, decreased the disparity between along- and across-track spacing, and allowed filtering on the basis of the standard deviations of the mean ice thicknesses.

Initial filtering involved the removal of gridded data points with only one contributing depth estimate. This removed a small amount of 1990s grid points that appeared to be due to errors in the navigation data.

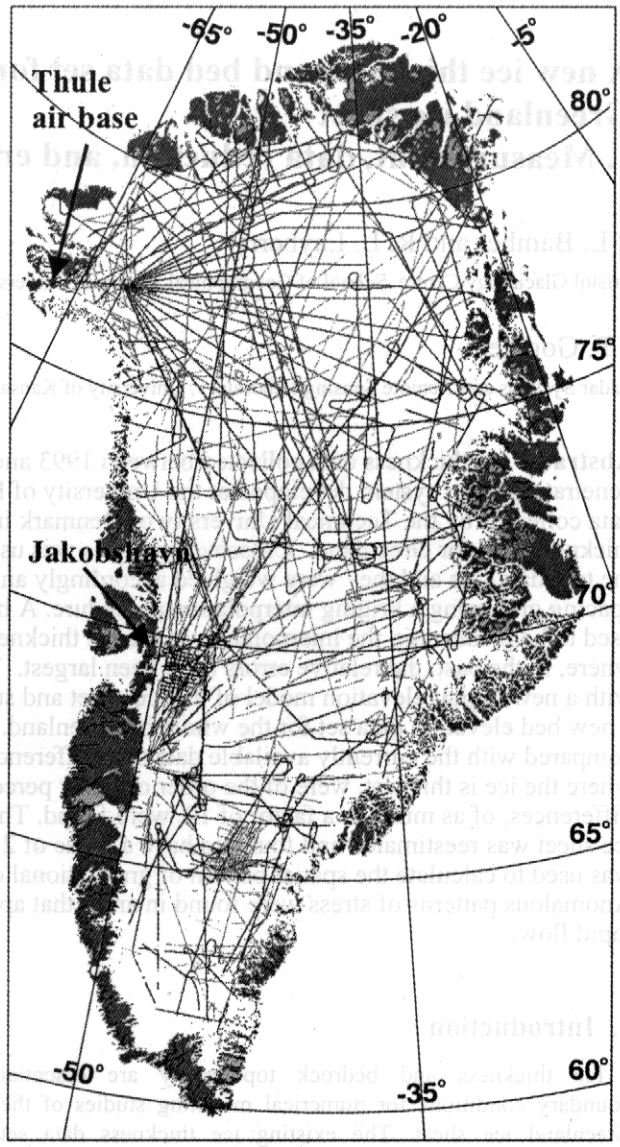

Figure 1. Airborne radar flight lines showing the coverage over the ice sheet. The 1990s data are shown as solid lines, and the 1970s data are plotted as shaded lines.

The average standard deviation in thickness at the grid points was 50 m, with the higher values being concentrated around the eastern ice sheet margin where the topography is the most extreme. Calculation of along-track standard deviations in thickness of the unaveraged data showed a strong correlation with the ice thickness, with the thinner ice having considerably greater standard deviations. Histograms of the standard deviations for different thickness bands gave distributions which were approximately Gaussian but with different widths. They also included points with anomalously high standard deviations that are potentially erroneous and were subsequently removed from the data. For each thickness band histogram, points that were <1% of the maximum value of the histogram were discarded. This removed 2% of the gridded data.

Much of the gridded data consisted of points wholly based upon depth estimates from either the 1990s or 1970s data and

this led to potential errors where less accurate 1970s data lay close to 1990s data. Results from the interpolation in this case (especially where flight lines from the different data sets are close to parallel) could give anomalously high local thickness gradients. At distances of three grid points (equivalent to 15 km) away from 1990s data, the errors in the 1970s data (taken to be roughly 130 m) would give an error in the bed slope of 0.5°, which was found, by trial and error, to be the maximum acceptable slope eror that would not adversely affect the kriged result. Gridded data points consisting entirely of 1970s data closer than three cells to 1990s data were removed to avoid introducing slope anomalies greater than this value. Finally, the coordinates of nonglacierized points at the edge of the ice sheet were appended to the mean x, y and z data, derived from a high-resolution (~2 km) land-ice mask [*Weng*, 1995], to provide a zero ice thickness boundary condition at the margins.

2.3 Interpolation

The quasi-regular grid of mean thicknesses was interpolated onto a 301 by 561 5-km grid. The interpolation approach used was that of kriging because of the great range in spatial density of data with which kriging copes well. Kriging is a form of weighted average estimator. The weights are assigned on the basis of the form of a model fitted to a function, in this case the variogram, which represents the spatial variability in the data [*Deutsch and Journel*, 1997]. The most commonly used form of kriging is ordinary kriging, where the sum of the weights is constrained to be equal to 1, and it is this form which was used here. The geostatistical properties of the data were obtained by computing a semivariogram. These can vary spatially and azimuthally over the data set. In this case, however, a single semivariogram was used in the kriging procedure. The sill was found to be 80 km. Beyond this distance the spatial correlation of the data is minimal. The variogram was estimated using the VARMAP software in the Geostatistical Library Software package [*Deutsch and Journel*, 1997]. This model is then used as input to the program KB2D from the same software package. The ice thickness grid that resulted from this interpolation procedure is shown in Figure 2.

Figures 3a and 3b show the standard deviation and the number of thickness values contributing to each mean point, respectively. These plots indicate the extent of the coverage after filtering. The standard deviations are a combination of the random error in the individual ice thickness measurements and the local variability in bed topography. Thus rougher areas will have a higher standard deviation, even though the accuracy of each shot is the same.

The pattern in Figure 3a, therefore, reflects the local roughness rather than variations in data accuracy. Highest standard deviations (and therefore roughness) are found toward the margins and, in particular, along the eastern side, with minima in the center of the ice sheet. This is discussed further by *Layberry and Bamber* [this issue] (paper 2). Figure 3b shows the number, n, of individual ice thickness measurements that contributed to each mean grid point. The 1970s data are evident as the points with the smallest values of n (black and dark gray lines). The kriging procedure generates an estimate of the variance of the fit of the data to the model it generates. This cannot be directly converted to an uncertainty in meters but does indicate the relative accuracy of the interpolated values and extrapolated values. The variance was also gridded at 5 km and may be of use for numerical modeling studies, as it is on the same grid as the thickness and indicates the relative reliability of each point. Minimum values for the uncertainty lie along 1990s tracks and have an error of ~10 m. Maxima lie in areas farthest from a track in areas of high thickness variability, and we estimate that the maximum uncertainty here is ~100 m.

3. Results and Discussion

The ice thickness grid was subtracted from a new digital elevation model (DEM) of the whole of Greenland [*Bamber et al.*, 2001] to produce a bed DEM. Figure 4 is a filled contour plot of this, highlighting, in particular, areas that are below

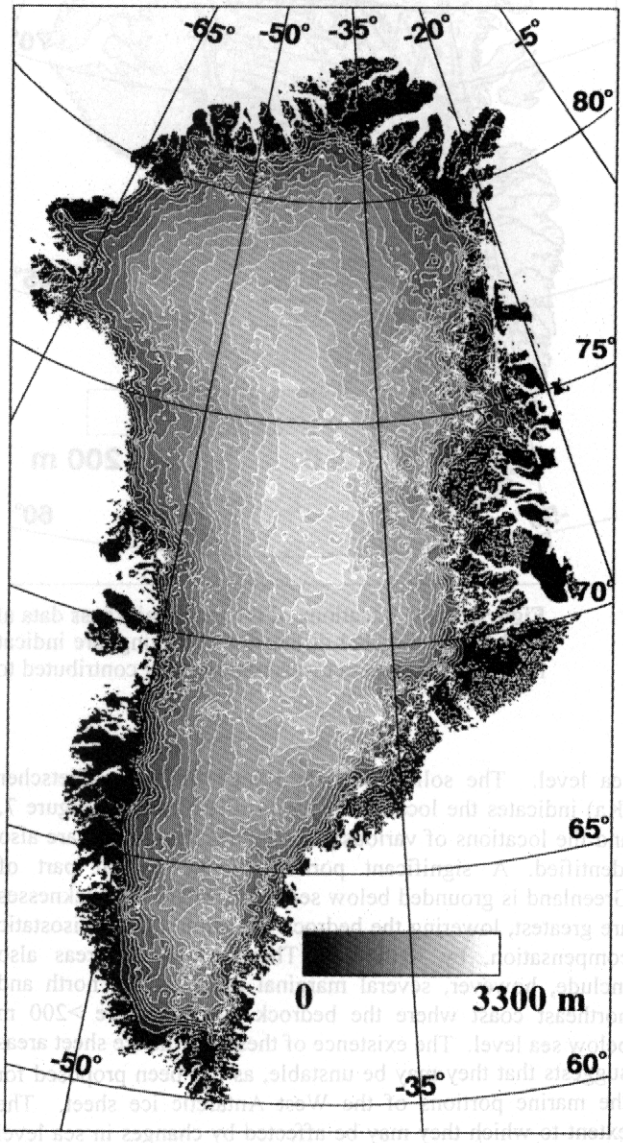

Figure 2. The ice thickness grid scaled between 0 and 3300 m. The maximum thickness computed was 3367 m. The land mask, used to constrain the thickness data at the ice edge, is shown sd solid, and the contour intervals used were 200 m.

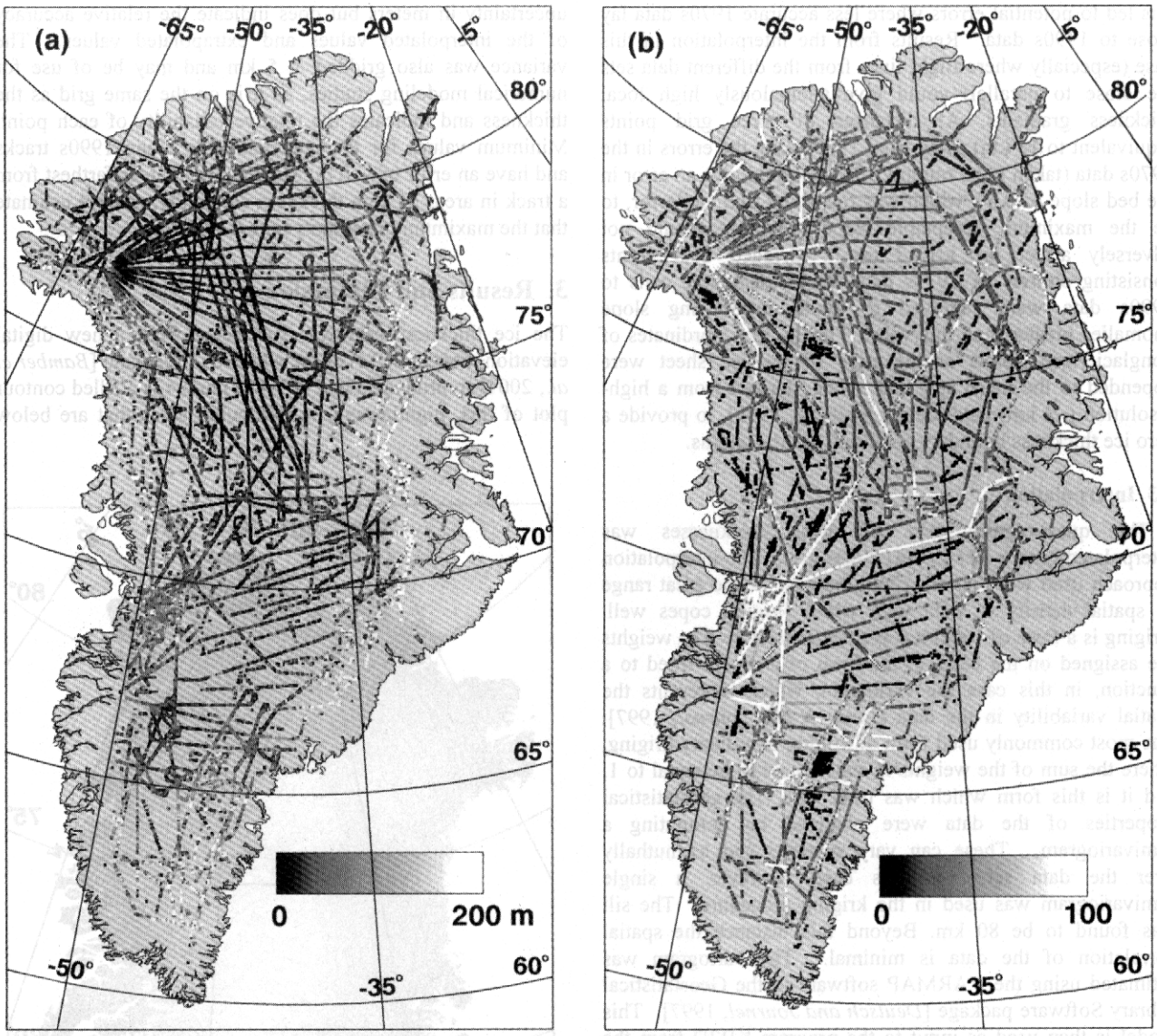

Figure 3. (a) Locations of the mean thickness data after the initial averaging step. The standard deviations of thickness, estimated during the averaging, are indicated by shades of gray ranging from 0 to 200 m. (b) The number of thickness measurements that contributed to each mean value.

sea level. The solid line near Kangerdlugssuaq Gletscher (Ka) indicates the location of the profile plotted in Figure 7, and the locations of various glaciers, discussed later, are also identified. A significant portion of the central part of Greenland is grounded below sea level, where ice thicknesses are greatest, lowering the bedrock elevation, through isostatic compensation, by ~1000 m. These low-lying areas also include, however, several marginal areas on the north and northeast coast where the bedrock elevations are >200 m below sea level. The existence of these marine ice sheet areas suggests that they may be unstable, as has been proposed for the marine portions of the West Antarctic ice sheet. The extent to which they may be affected by changes in sea level and/or ice thickness was investigated by examining how close to floatation they are. Assuming values of sea water density and estimating average ice column density [*Bamber and Bentley*, 1994], it is possible to compute how much in excess of the floatation thickness an ice column is. Taking ice thickness profiles along Humboldt Gletscher, the "excess thickness" rises rapidly to 500 m within 25 km from the ice edge. Petermann Gletscher has a floating tongue, and, upstream of this, the "excess", as previously, rises rapidly to ~500 m within about the same distance. A similar picture emerges for the northeast Greenland ice stream (NEGIS). From this it is inferred that these regions have high enough ice thickness gradients to make them insensitive to short-term changes in either sea level or ice thickness.

We have made a simple estimate of what the unloaded bed elevations would be in the absence of the ice sheet (assuming mean densities of 3370 kg m^{-3} and 910 kg m^{-3} for the mantle and ice, respectively, so that the amount of uplift is 910/3370 times the ice thickness). This is shown in Figure 5. The low-lying areas around Humboldt and Petermann Gletschers and the NEGIS are still below sea level by as much as 200 m. Without the overlying ice, central Greenland, however, lies substantially above sea level and is remarkably flat. The

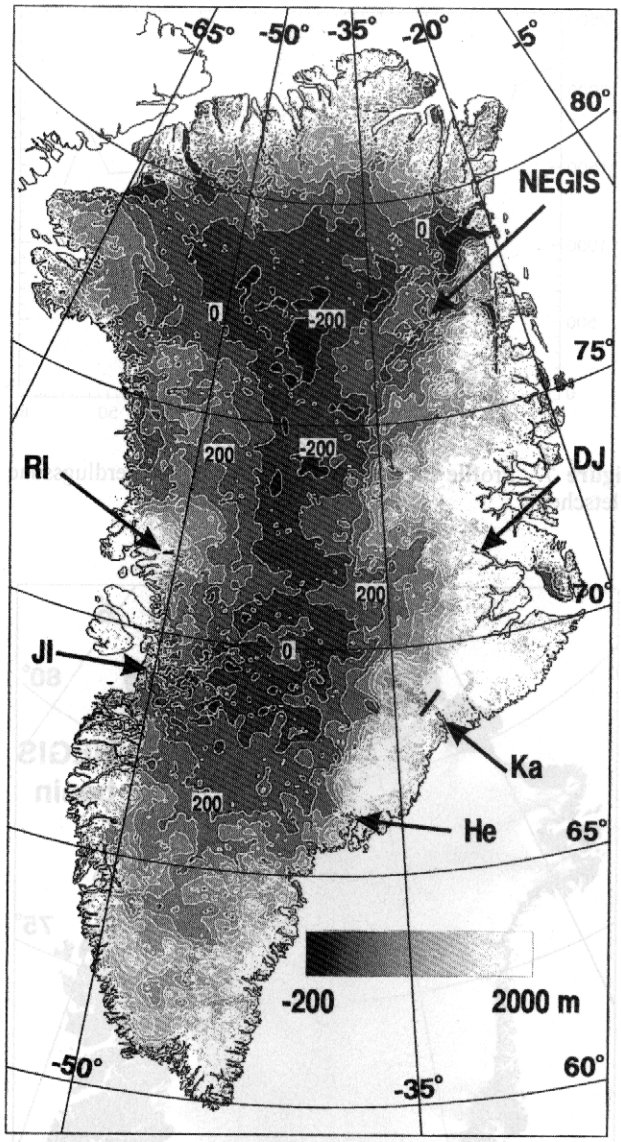

Figure 4. The bed elevations calculated by subtracting the ice thickness grid from a new digital elevation model of Greenland [*Bamber et al.*, 2001]. The contour interval used was 200 m. The first three contour intervals have been labeled. Abbreviations for glaciers are as follows: NEGIS, northeast Greenland ice stream; RI, Rinks Isbræ; JI, Jakobshavn Isbræ; DJ, Daugaard Jensen; Ka, Kangerdlugssuaq; and He, Helheim.

elevation change over a distance of 2500 km running north-south is just 300 m ranging from ~500-800 m above sea level. Higher elevations and larger variations are only found for the southern tip of the island and a section along the east coast.

One of the most striking features in Figure 4 is the deep channel running from the center toward the northeast coastline (in the vicinity of the NEGIS). Figure 6 is a plot of balance velocities for the ice sheet (discussed further in paper 2), which are an estimate of the depth-averaged velocity field. They were calculated from a recent compilation of accumulation (F. Jung-Rothenhäusler et al., Greenland accumulation distribution: a GIS-based approach, submitted to *Journal of Glaciology*, 1999), a new 1-km DEM mentioned earlier [*Bamber et al.*, 2001], and the ice thickness grid presented here. A two-dimensional finite difference scheme [*Budd and Warner*, 1996] was used in preference to the more traditional flow line approach. The balance velocities shown in Figure 6 are identical to those presented in an earlier paper [*Bamber et al.*, 2000a] with one important exception. In the previous study, ablation was not correctly accounted for, resulting in balance velocities that were too high below the equilibrium line of the ice sheet. Here we have corrected this error using a positive degree day model and parameters described elsewhere [*Huybrechts et al.*, 1991]. It is evident that the deep channel in Figure 4 coincides with the existence of the NEGIS, and, therefore, it seems likely that basal topography plays a key role in determining the position and existence of this feature. This is discussed by *Joughin et al.* [this issue] and *Layberry and Bamber*, [this issue]. This feature can also be seen in a difference plot of the new and Letreguilly grids, indicating that the trough was not captured in the latter. This may partly explain why the northeast ice stream is not present in any numerical simulations of the dynamics of the whole ice sheet [*Bamber et al.*, 2000b].

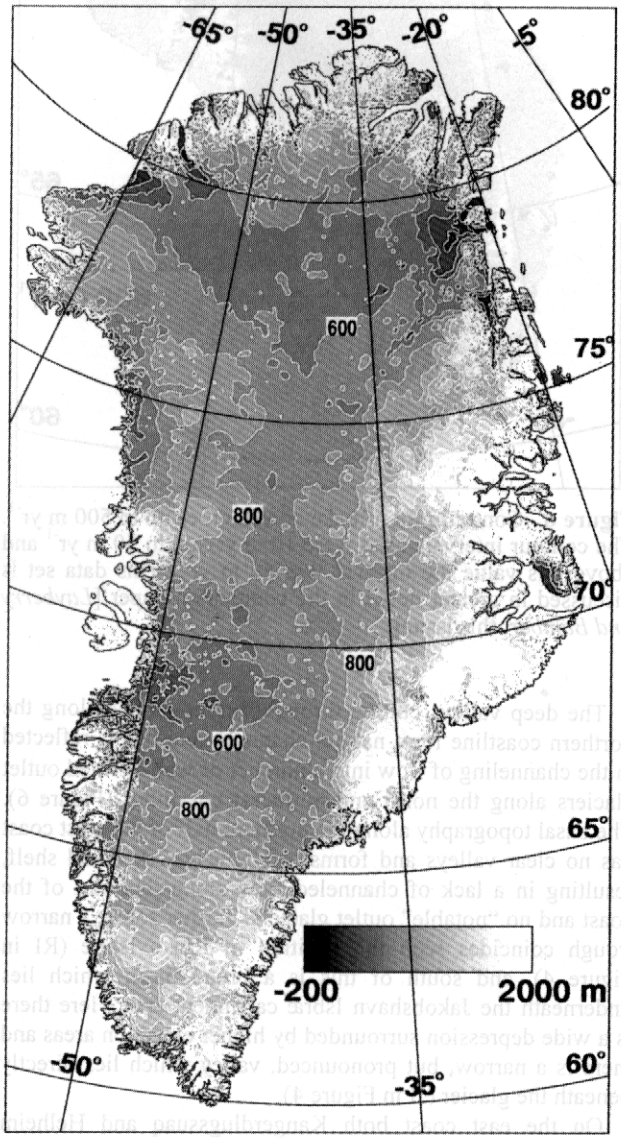

Figure 5. Bed elevations compensated for the removal of the ice sheet.

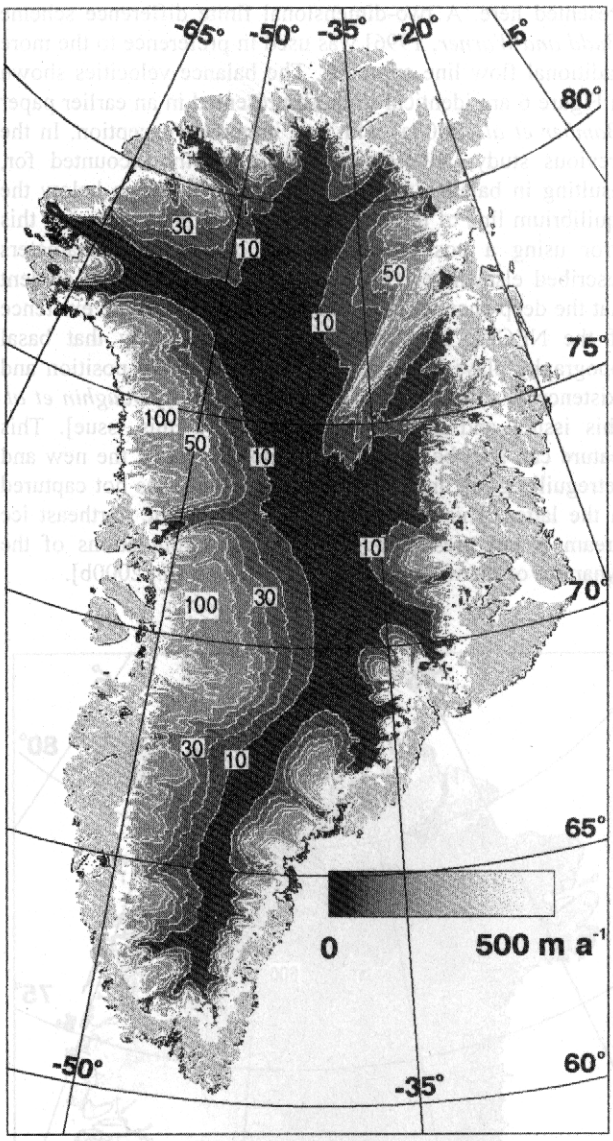

Figure 6. Contour plot of balance velocities up to 500 m yr^{-1}. The contour intervals used were 10 m yr^{-1} up to 50 m yr^{-1} and above this value the interval was 50 m yr^{-1}. This data set is discussed in greater detail in the companion paper [*Layberry and Bamber*, this issue].

The deep valleys cutting through the mountains along the northern coastline form natural channels, and this is reflected in the channeling of flow into a number of well-defined outlet glaciers along the north and northeast coastlines (Figure 6). The basal topography along the northern half of the west coast has no clear valleys and forms a relatively flat, broad shelf, resulting in a lack of channeled flow along this part of the coast and no "notable" outlet glaciers. Farther south, a narrow trough coincides with the position of Rinks Isbræ (RI in Figure 4), and south of this is a broad basin which lies underneath the Jakobshavn Isbræ catchment area. Here there is a wide depression surrounded by higher elevation areas and there is a narrow, but pronounced, valley which lies directly beneath the glacier (JI in Figure 4).

On the east coast both Kangerdlugssuaq and Helheim Gletschers (Ka and He in Figure 4) lie in deep valleys surrounded by mountainous terrain on either side. Both of

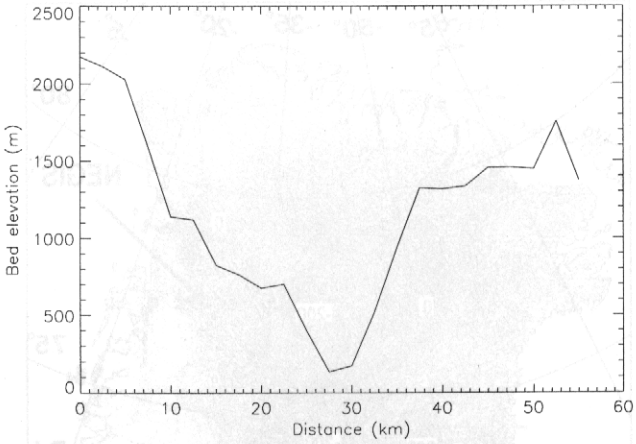

Figure 7. Profile of bed elevation across Kangerdlugssuaq Gletscher.

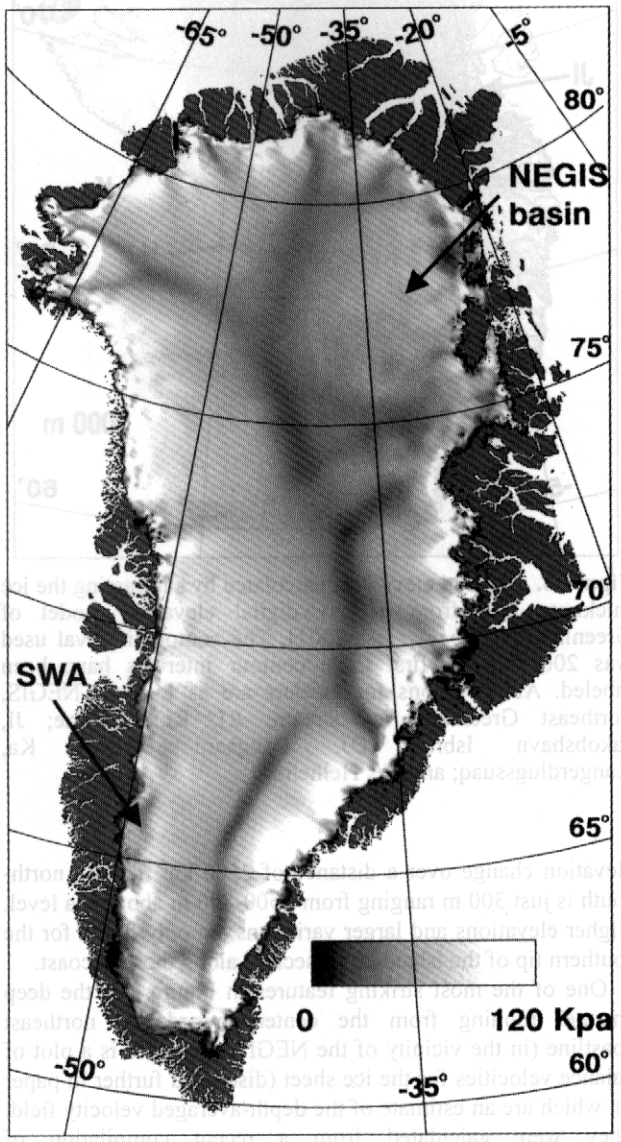

Figure 8. Plot of gravitational driving stress calculated with the aid of the new ice thickness grid. The range is from 0 to 120 kPa, and the two anomalous areas, southwest (SWA) and NEGIS, are marked.

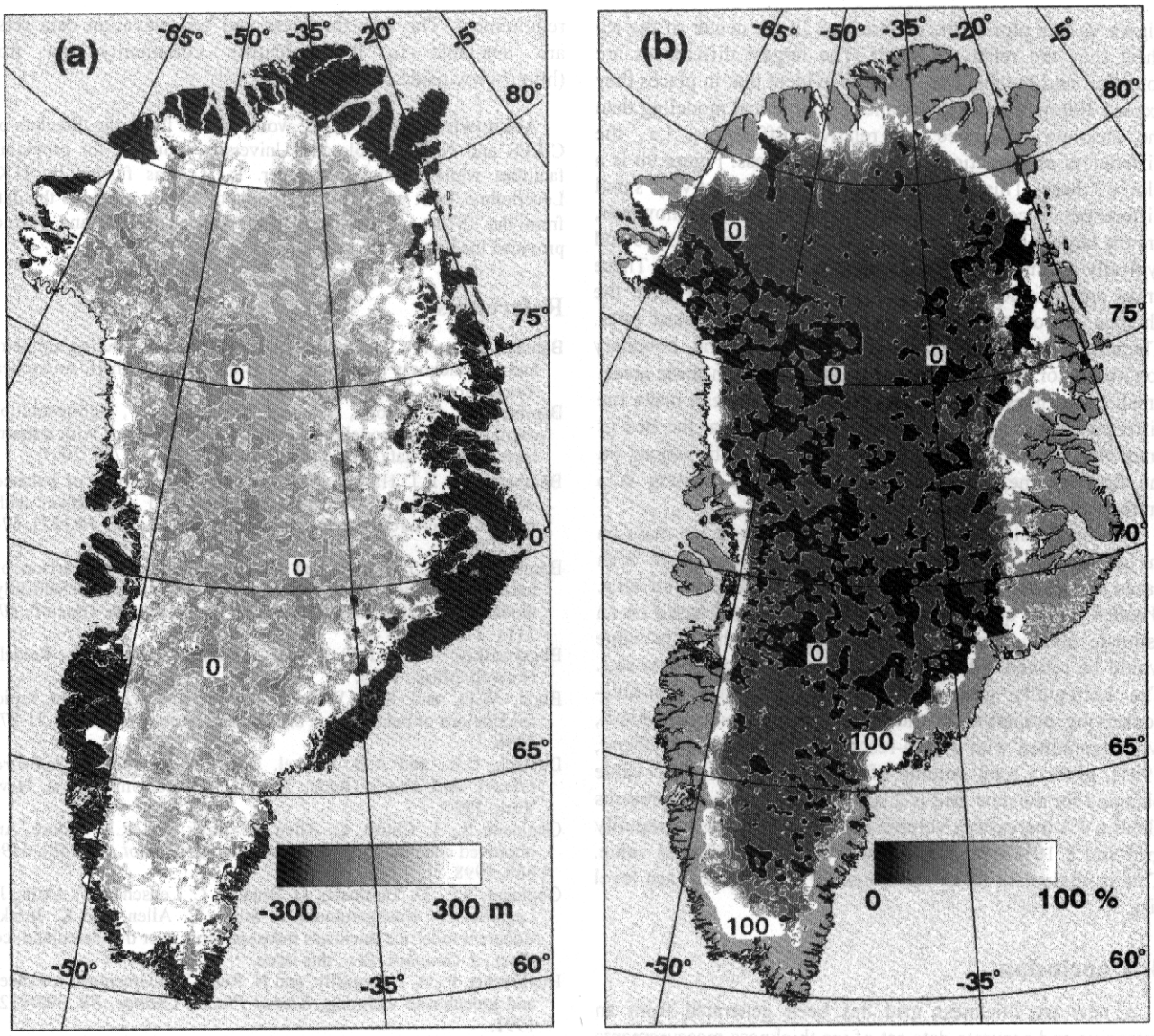

Figure 9. (a) The difference between the Letreguilly grid and the new ice thickness grid (z_{new}-$z_{letreguilly}$). (b) The ratio of the difference of ice thickness plotted in 9a and $z_{letreguilly}$ (z_{new}-$z_{letreguilly}$/$z_{letreguilly}$). The regions of largest relative difference around the margins are particularly apparent as open areas in this plot. The contour interval used here was 0.2, and it is clear that for much of the ice sheet interior the two data sets agree to within 20%.

these glaciers display channeled flow with high velocities (>1 km yr^{-1}) (Figure 6). Figure 7 is a profile across the mouth of Kangerdlugssuaq Gletscher. The location of the profile is shown by the solid line in Figure 4. The elevation ranges from near sea level to ~2200 m in a distance of just 25 km, which equates to a slope of 4.3°. From the discussion above, it can be seen that the bedrock topography appears to dictate the pattern of discharge seen in Figure 6. Ice sheet flow is driven by the gravitational driving stress

$$\tau = -\rho g z \sin\alpha \quad (1)$$

where ρ is the density of ice and g is the gravitational constant, z is the ice thickness, and α is the surface slope. The value of α was estimated from the new DEM of Greenland [*Bamber et al.*, 2001] smoothed over 20z. The pattern of driving stress is shown in Figure 8.

The spatial pattern is fairly uniform, reflecting the increase in surface slope moving away from the ice divides toward the coast, with maximum values at the margins of the ice sheet. The exception to this pattern is the basin containing the NEGIS. In this basin the trend is much less clear, and values at the margin are noticeably less than for the other basins. There is also a region near the margin in the southwest (SWA in Figure 8) that also seems to have anomalously low shear stress when compared with the pattern for other basins. The estimates of driving stress shown in Figure 8 are used in paper 2 to differentiate between different types of flow regime. We note here, however, that the basin containing the NEGIS and an area in the southwest appear to be anomalous in terms of the spatial pattern and magnitude of driving stresses toward the ice edge.

The differences between the new grid and the one in current use [*Letreguilly et al.*, 1991] have been investigated.

Figure 9a is a plot of the differences. In the center of the ice sheet they are relatively small. The largest differences are found around the margins, and it is evident that in places they exceed 300 m. Of more relevance to numerical modeling than the absolute difference are relative differences, i.e., the differences as a fraction of the total thickness. Figure 9b is a plot of these. This plot also highlights the relatively small differences in central Greenland. Of more interest, however, are the large relative differences (as much as a factorof 10 and typically a factor of 5) near the margins of the ice sheet. These areas are the most dynamically "sensitive". They have the shortest response time and are flowing at the fastest rates. Therefore, it is particularly important that the boundary conditions for numerical modeling are reliable in these areas. Small differences in thickness in these regions can make the difference between a model predicting melting at the bed or predicting a frozen bed. This can have a dramatic impact on the flow regime [*Bamber et al.*, 2000b], as melting is a prerequisite for basal sliding.

The Greenland ice sheet is the second largest ice mass on the planet, and previous estimates of its volume have been based on earlier IPR measurements of thickness and area. *Weidick* [1995] quotes a value of 2.6×10^6 km^3 based on an estimate obtained in the 1950s, suggesting that this value would be refined with the acquisition of improved data sets. The Letreguilly grid (after correcting for the non-area-conserving properties of the polar stereographic projection), when combined with a high-resolution land-ice mask [*Weng*, 1995], gives a total volume of 2.809×10^6 km^3. The value obtained for the new grid is 2.931×10^6 km^3, which represents about a 4% increase in volume compared with the Letreguilly grid and a 10% increase on the previously published value. This is equivalent to an additional 70 cm of global sea level rise.

4. Conclusion

A new ice thickness grid has been generated from an extensive and accurate data set of ice thickness measurements collected during the 1990s by the University of Kansas. The new grid has been combined with a new digital elevation model of Greenland to derive a bed DEM. Comparing this with balance velocity estimates for the ice sheet reveals how the bed topography controls the pattern of flow over the ice sheet, and this is particularly apparent for the northeast ice stream. The presence of this feature is clearly associated with a distinct basal trough. Driving stresses calculated from the new ice thickness grid for the basin containing the northeast ice stream appear to be anomalous both in their spatial pattern and magnitude when compared with other basins. Large differences between the data set currently in use and the one presented here were found within a region of about 50-200 km from the ice sheet margin. We believe that these differences will have a significant impact on the simulations of ice sheet dynamics produced by numerical models. Of particular relevance for modeling is knowledge of the uncertainty in the input data. The spatial pattern of variance for each grid point has been generated to satisfy this requirement. The new thickness and bed elevation data sets are available to the scientific community via ftp (http://www.nsidc.org).

Acknowledgments. J.L.B. would like to thank the directors of CIRES and NSIDC, Colorado University, Boulder, for providing facilities while writing this paper. R.L.L. was funded by U.K. Leverhulme Trust grant F/182/BJ. Simon Ekholm provided the data from the 1970s and the land-ice mask used and Roland Warner provided the balance velocity code.

References

Bamber, J.L., and C.R. Bentley, A comparison of satellite altimetry and ice thickness measurements of the Ross ice shelf, Antarctica, *Ann. Glaciol.*, *20*, 357-364, 1994.

Bamber, J.L., S. Ekholm, and W.B. Krabill, A new, high-resolution digital elevation model of Greenland fully validated with airborne laser altimeter data, *J. Geophys. Res.*, *106*, 6733-6745, 2001.

Bamber, J.L., R.J. Hardy, and I. Joughin, An analysis of balance velocities over the Greenland ice sheet and comparison with synthetic aperture radar interferometry., *J. Glaciol.*, *46*(152), 67-72, 2000a.

Bamber, J.L., R.J. Hardy, and H. Huybrechts, A comparison of balance velocities, measured velocities and thermomechanically modelled velocities for the Greenland Ice Sheet, *Ann. Glaciol.*, *30*, 211 – 216, 2000b.

Bogorodskiy, V., and C. Bentley, *Radioglaciology*, D. Reidel, Norwell, Mass., 1985.

Budd, W.F., and R.C. Warner, A computer scheme for rapid calculations of balance-flux distributions, *Ann. Glaciol. 23*, 21-27, 1996.

Deutsch, C.L., and A.G. Journel, *GSLIB. Geostatistical Software Library and User's Guide*, 2nd ed., Oxford Univ. Press, New York, 1997.

Gogineni, S., T. Chuah, C. Allen, K. Jezek, and R.K. Moore, An improved coherent radar depth sounder, *J. Glaciol.*, *44*(148), 659-669, 1998.

Gogineni, S.P., D. Tammana, D. Braaten, C. Leuschen, T. Akins, J. Legarsky, P. Kanagaratnam, J. Stiles, C. Allen, and K. Jezek, Coherent radar ice thickness measurements over the Greenland ice sheet., *J. Geophys. Res.*, this issue.

Huybrechts, P., A. Letreguilly, and N. Reeh, The Greenland ice sheet and greenhouse warming, *Global Planet. Change*, *89*, 399-412, 1991.

Joughin, I., M. Fahnestock, D. MacYeal, and J.L. Bamber, Observation and analysis of ice flow in the largest Greenland ice stream, *J. Geophys. Res.*, this issue.

Layberry, R., and J.L. Bamber, A new ice thickness and bed data set for the Greenland ice sheet 2, Relationship between dynamics and basal topography, *J. Geophys. Res.*, this issue.

Letreguilly, A., P. Huybrechts, and N. Reeh, Steady-state characteristics of the Greenland ice-sheet under different climates, *J. Glaciol.*, *37*(125), 149-157, 1991.

Weidick, A., Greenland, in *Satellite Image Atlas of Glaciers of the World*, edited by R.S. Williams and J. Ferrigno, p. 141, U.S. Geol. Surv., Washington, D.C., 1995.

Weng, W.L., Untitled, *Arctic*, *48*(2), 206-206, 1995.

J. L. Bamber and R. L. Layberry, Bristol Glaciology Centre, School of Geographical Sciences, University of Bristol, University Road, Bristol, BS8 1SS, England, U.K. (j.l.bamber@bristol.ac.uk; r.layberry@bristol.ac.uk)

S. P. Gogineni, Radar Systems and Remote Sensing Laboratory, The University of Kansas, 2291 Irving Hill Road, Lawrence, KS 66045. (gogineni@rsl.ukans.edu)

(Received August 4, 2000; revised December 15, 2000; accepted January 11, 2001.)